

# Goos–Hänchen and Imbert–Fedorov shifts for leaky guided modes

Frank Pillon, Hervé Gilles, Sylvain Girard, and Mathieu Laroche

*Equipe Lasers, Instrumentation Optique et Applications, Centre Interdisciplinaire de Recherche Ions Laser, Centre National de la Recherche Scientifique-Commissariat à l’Energie Atomique-Ecole Nationale Supérieure d’Ingénieurs de Caen Unité Mixte de Recherche (UMR 6637), 6 boulevard du Maréchal Juin, 14050 Caen Cedex, France*

Robin Kaiser

*Institut Non Linéaire de Nice, Centre National de la Recherche Scientifique/Unité Mixte de Recherche (UMR 6618), 1361 route des Lucioles, F-06560 Valbonne, France*

Azra Gazibegovic

*Prirodno Matematički Fakultet, Zmaja od Bosne 53, 71000 Sarajevo, Bosnia-Herzegovina*

Received October 27, 2004; revised manuscript received December 17, 2004; accepted December 29, 2004

The Goos–Hänchen shift for a light beam totally reflected on the external interface of a dielectric thin film deposited on a high-index substrate can be strongly enhanced through some specific incidence angles corresponding to the leaky guided modes into the layer. Because the resonant eigenstates are polarization dependent, it has been possible to observe such resonance with an experimental setup based on a periodic modulation of the polarization state combined with position-sensitive detection. Classical models usually used for a single interface (Artmann’s model based on phase argument and Renard’s model based on an energetic interpretation) have been re-adapted to describe the behavior of the entire layer. Good agreement is obtained between theory and experimental results. © 2005 Optical Society of America

*OCIS codes:* 240.6690, 260.6970, 230.3720.

## 1. INTRODUCTION

The Goos–Hänchen (GH) shift<sup>1</sup> is the small displacement that a light beam undergoes when it is totally reflected on the interface separating two infinite half-spaces, one with a higher refractive index than the other. Such spatial shift is attributed to the evanescent wave that travels along the interface. It appears as if the incident light penetrates first into the lower-refractive-index medium as an evanescent wave before being totally reflected back into the high-index space. If we consider such physical interpretation, the GH effect appears as clear experimental evidence that the ray model is simply a first approximation, and that only the wave approach could allow a complete description of the total reflection. The order of magnitude of the GH shift during a total internal reflection in the optical domain is relatively small (typically of the order of the wavelength, i.e., a few micrometers in the visible or near infrared) and is therefore difficult to observe experimentally after a single total reflection. However, despite the difficulties, several original techniques have been developed for an experimental observation of this fundamental optical effect. The most common method consists of using multiple reflections in a slab<sup>2</sup> or a prism<sup>3</sup> structure to increase the shift by a factor corresponding to the number of successive reflections. But this allows relatively poor control of the spatial beam geometry along the different reflections, which is a disadvantage when the

experimental results are compared to theoretical models. More recently, enhancement of the effect has been obtained as a result of total internal reflection inside a laser cavity.<sup>4</sup> Despite this technique’s being a very original approach to the problem of measuring the GH shift after a single total reflection, it appears complicated to modify the incidence angle, as it is necessary to realign the entire isotropic cavity between measurements.

Our group has developed a totally different approach aimed at the improvement of the optical detection sensitivity to very small spatial shifts of a light beam. It is based on the use of a special shaped photodiode called a position-sensitive detector (PSD) and on a periodic switching between two orthogonal states by use of an electro-optic modulator (Pockels cell or liquid-crystal valve (LCV)). This technique was first used to measure precisely the longitudinal GH shift<sup>5</sup> versus the angular incidence when the polarization states switch between TE and TM. More recently, the Imbert–Fedorov<sup>6</sup> (IF) shift, which corresponds to a transverse displacement perpendicular to the incident plane, was also precisely measured when the polarization states were switched periodically between left and right circular states.<sup>7</sup> Until now, the technique has been used only to measure the geometrical shifts after a total reflection on a single dielectric interface.

It has also been pointed out in earlier works on the GH

shift that peculiar behavior could also be observed when total reflection occurs on structures containing multiple dielectric layers.<sup>8,9</sup> One of the interesting cases involves a simple guiding structure formed by a substrate with a high refractive index covered by a single dielectric layer with a low refractive index. If the incident angle inside the substrate is correctly chosen to obtain refraction on the substrate–layer interface and total reflection on the layer–air interface, some resonance could appear on the GH shift for a discrete series of specific angles.<sup>10</sup> This behavior has already been investigated because it represents interesting opportunities to make atomic mirrors<sup>11</sup> or optical sensors.

The present paper is devoted to a full reinvestigation of the interesting properties of such guiding structure with our original experimental setup. It is divided into three main parts. The first part contains a theoretical description of the GH shift on a single dielectric layer. Different models initially developed to describe the total reflection on a single interface—such as Artmann’s model<sup>12</sup> based on a phase argument or Renard’s model<sup>13</sup> based on an energetic approach—have been modified to take into account the effect of the dielectric layer. This major revision will be complemented by some comments on important parameters that could influence the resulting displacement, such as the distributed losses into the layer.

The second part of the paper is dedicated to a description of the experimental results obtained on a single dielectric layer with our setup based on both periodic polarization switching and PSD detection. The main experimental results are obtained in the case of polarization switching between TE and TM states, because these two states correspond naturally to the polarization eigenstates of a planar waveguide. The experimental GH shifts are then compared with the theory, and some comments are offered on the observed resonance. Complementary measurements are also reported on the experimental observation of the transverse IF shift in such structure. The different parameters (thickness, losses, refractive index of the substrate or the thin-film, etc.) that could have a significant influence on the effect of resonance observed in the layer used here are discussed.

Finally the conclusion deals with future possible applications for such components based on the observation of modification of the resonance. Other original structures presenting a potentially enhanced Goos–Hänchen shift will be briefly reviewed and the opportunity to study such systems with our experimental technique will be discussed.

## 2. THEORETICAL MODELS OF THE GOOS–HÄNCHEN SHIFT ON A SINGLE DIELECTRIC LAYER

In the past two main models have been investigated to describe accurately the GH or IF shifts observed after a total internal reflection on a dielectric interface. The first approach, usually called Artmann’s model,<sup>12</sup> is based on an argument considering the phase shift of the reflected beam with respect to the incident beam. To summarize the main results obtained with Artmann’s model, we can limit our discussion to the particular case of an incident

beam well collimated with a divergence of only a few milliradians. In this case the GH effect corresponds simply to a displacement  $L_{\text{GH}}$  along the interface of the incident plane (see Fig. 1) that is given by

$$L_{\text{GH}} = \frac{\lambda}{2\pi n_1 \cos i_1} \left( \frac{d\Phi}{di_1} \right), \quad (1)$$

where  $\lambda$  is the wavelength in vacuum,  $n_1$  is the refractive index of the substrate,  $\Phi$  is the phase shift during the total reflection for an incident plane wave, and  $i_1$  is the incidence angle.

The second approach, usually called Renard’s model,<sup>13</sup> is based on an argument with respect to the energy flow of the evanescent wave along the interface. As already reported elsewhere (see for example the explanation detailed in Ref. 7) the GH displacement  $L_{\text{GH}}$  on the interface may be expressed as

$$L_{\text{GH}} = \frac{1}{\langle \Sigma_{\text{rx}} \rangle} \int_{-\infty}^0 \langle \Sigma_{\text{tz}} \rangle dx, \quad (2)$$

where  $\Sigma_{\text{rx}}$  is the Poynting’s vector component for the reflected beam along the axis normal to the interface and  $\Sigma_{\text{tz}}$  is the Poynting’s vector component for the evanescent wave along the axis aligned on the interface and in the incident plane. The Poynting’s vectors are time averaged (symbol  $\langle \rangle$ ).

### A. Adaptation of Artmann’s Model for a Single Dielectric Layer

The layer structure investigated during the present work consists of a thin, homogeneous dielectric film of thickness  $h$  and refractive index  $n_2$  deposited on a substrate with a refractive index  $n_1$  (see Fig. 2). The index of the substrate  $n_1$  is higher than the index of the thin film  $n_2$ . There is no cladding covering the thin film and the medium above the layer is simply air, which could be considered a dielectric medium with a refractive index  $n_3$  of 1. The incident light is injected through the substrate into the thin film thanks to a specifically designed prismatic structure for the substrate as shown in Fig. 3(a). If we follow an approach similar to Artmann’s model already mentioned for a single interface, we can calculate the spatial shift that results from the phase shift  $\Phi$  between the incident and the reflected waves. The amplitude of the total

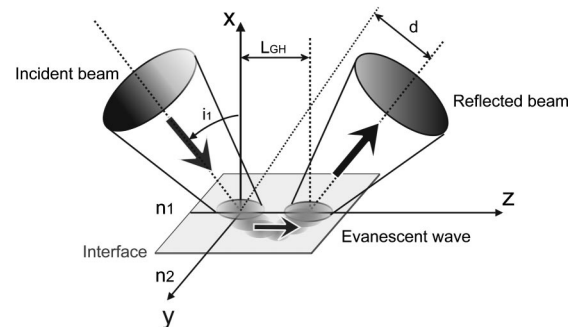


Fig. 1. Schematic representation of the Goos–Hänchen effect as a pure spatial shift for the reflected light beam. This simplified representation is correct when the incident beam has low divergence.

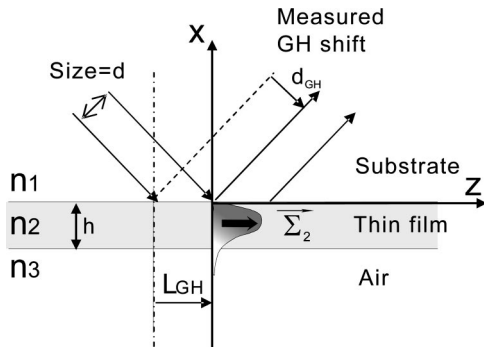


Fig. 2. Size of the incident beam  $d$  adjusted exactly such that the spatial shift corresponds to an incident beam that completely penetrates into the lower-refractive-index medium as an evanescent wave (Renard’s model).

reflection coefficient for the entire system (the two interfaces and the homogeneous film) is classically calculated by an approach similar to that used in the case of a Fabry–Perot interferometer [see Fig. 3(b)]. The amplitude of the complex reflection coefficient is described as

$$r_{\text{tot}} = r_{12} + \frac{t_{12}t_{21}r_{23} \exp(j\varphi)}{1 - r_{21}r_{23} \exp(j\varphi)} = |r_{\text{tot}}| \exp(j\Phi), \quad (3)$$

where  $r_{ij}$  represents the reflection coefficient for the interface separating media  $i$  and  $j$ ,  $t_{ij}$  is the corresponding transmission coefficient, and  $\varphi$  is the phase shift between two successively reflected waves due to the optical path difference for a round trip into the layer. The reflection  $r_{ij}$  and transmission  $t_{ij}$  coefficients are related to the refractive index  $n_i$  and  $n_j$  and to the incidence angle  $i_1$  according to the classical Fresnel formulas.<sup>14</sup> The phase shift  $\varphi$  depends on the thickness  $h$  of the layer, its refractive index  $n_2$ , and the refracted angle  $i_2$  into the layer, as well as the wavelength  $\lambda$  according to

$$\varphi = \frac{2\pi n_2}{\lambda} 2h \cos i_2. \quad (4)$$

The complex nature of the total reflection coefficient is due simultaneously to the total reflection on the second interface described by the complex coefficient  $r_{23}$  and to the interference term that is directly related to the  $\varphi$  value. If we start with Eq. (3), it is straightforward to calculate numerically the argument of the complex coefficient  $r_{\text{tot}}$ . This argument  $\Phi$  corresponds to the total phase shift that could be inserted into Eq. (1) to simulate the GH shift for the thin film by use of Artmann’s model. Of course the second part of Eq. (3) contains the interference term and therefore represents possible resonance effects that depend on the incidence angle.

Furthermore the complex reflection coefficient is polarization dependent with two polarization eigenstates (TE, with an electric field perpendicular to the incident plane, and TM, with a magnetic field perpendicular to the incident plane). This is because the dephasing factor during the total reflection on the film–air interface depends on the polarization states. Therefore the resulting GH displacement will also be slightly dependent on the polarization states. The difference  $\Delta L_{\text{GH}}$  between the displacements for TE and TM states is equal to the amplitude of

periodic spatial movement along the substrate–film interface when the polarization state of the incident beam is periodically switched between TE and TM. It can be expressed as

$$\Delta L_{\text{GH}} = \frac{\lambda}{2\pi n_1 \cos i_1} \left[ \left( \frac{d\Phi^{\text{TE}}}{di_1} \right) - \left( \frac{d\Phi^{\text{TM}}}{di_1} \right) \right], \quad (5)$$

where  $\Phi_{\text{TE}}$  and  $\Phi_{\text{TM}}$  are respectively the arguments of the total reflection coefficients for TE and TM modes, and the other parameters correspond to those used in Eq. (1). Our experimental setup allows measuring  $\Delta d_{\text{GH}}$ . The difference  $\Delta L_{\text{GH}}$  is directly deduced following  $\Delta L_{\text{GH}} = \Delta d_{\text{GH}} / \cos i_1$  (see Fig. 2).

### B. Adaptation of Renard’s Model for a Single Dielectric Layer

For Renard’s model the electromagnetic waves propagating in the film and in the air are considered a single, inhomogeneous electromagnetic field distribution. Renard’s formula can be presented as

$$L_{\text{GH}} = \frac{1}{\langle \Sigma_{\text{rx}} \rangle} \left( \int_{-h}^0 \langle \Sigma_{2z} \rangle dx + \int_{-\infty}^{-h} \langle \Sigma_{3z} \rangle dx \right), \quad (6)$$

where  $L_{\text{GH}}$  represents the absolute longitudinal shift along the substrate–film interface compared with the position of the incident beam,  $\Sigma_{\text{rx}}$  corresponds to the component along the  $x$  axis of the Poynting’s vector for the reflected beam inside the substrate,  $\Sigma_{2z}$  is the component along the  $z$  axis of the Poynting’s vector for the guided wave inside the film, and  $\Sigma_{3z}$  is also the component along the  $z$  axis of the Poynting’s vector, but for the evanescent

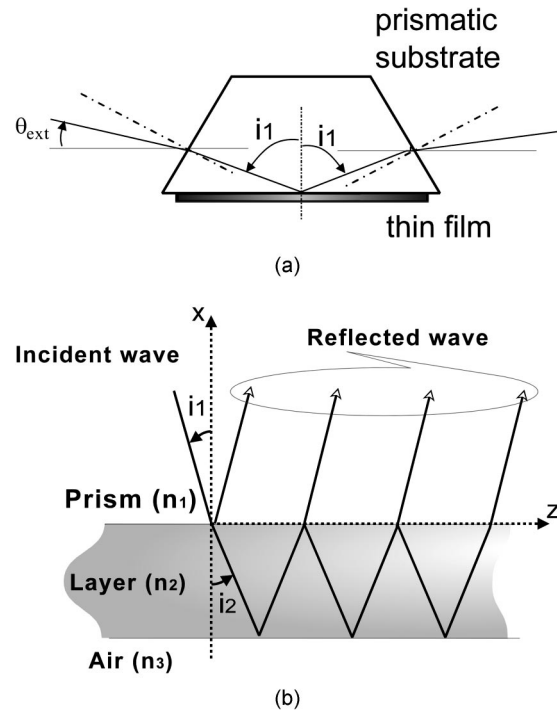


Fig. 3. Schematic representation of the thin layer deposited on a substrate: (a) the prismatic structure of the substrate, (b) the reflected wave that can be calculated with an approach similar to the one usually used in Fabry–Perot interferometer with the multiple reflections into the thin film.

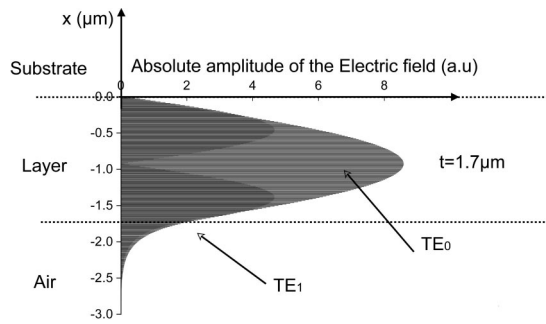


Fig. 4. Calculated electric field distribution inside the guiding structure for  $TE_0$  and  $TE_1$  modes.

wave in the air. Therefore because Renard's model is entirely based on the expression of the Poynting's vectors, it becomes necessary to determine completely the expression of the electromagnetic field in the substrate, the film, and the air. In the film the electromagnetic wave results from the superposition of two counterpropagating waves. One wave propagates in the direction of the incident beam while the second corresponds to a wave backreflected by the film–air interface. As in the case of any optical waveguide, each eigenmode can be considered a standing wave along the transverse  $x$  axis and a propagating wave along the longitudinal  $z$  axis. Moreover, the incidence angle  $i_1$  should satisfy specific conditions to produce a well-controlled standing wave along the  $x$  axis. However, in the present system there is no total internal reflection on the interface between the film and the substrate; consequently the eigenmodes are progressively radiated back into the substrate. Therefore these eigenmodes are progressively attenuated along the  $z$  axis even without any losses into the waveguide. For this reason they can be considered leaky guided modes.

Of course, as soon as a guiding effect into the film appears, the GH displacement will be enhanced. As already described in the previous paragraph, the effect is polarization dependent. Therefore it is necessary to distinguish the effect that depends on the incident polarization state. Different expressions must be established for a complete description of the electric and magnetic fields reflected into the substrate, or injected into the thin film and into the air (See Appendix A for the expression of the reflected and evanescent waves and Appendix B for the guided field into the thin layer). The expressions for the electric field distribution inside the dielectric layer and in the air are dependent on the incidence angle. As soon as this incidence angle corresponds to a resonance, the amplitude of the electric field inside the thin dielectric layer becomes enhanced. Starting with an incidence angle corresponding to the critical angle for the layer–air interface, the different resonant modes appear as the angle  $i_1$  is increased. The first resonance corresponds to  $TE_0$ , the second to  $TE_1$ , and so on for a TE incident polarized beam.

As examples, two electric field distributions were calculated for  $TE_0$  and  $TE_1$  respectively and are illustrated in Fig. 4. The amplitude of the electric field is significantly enhanced compared with the amplitude into the substrate when the light is guided into the structure.

Appendixes A and B also contain the detailed expressions for Poynting's vectors. From these expressions, it

becomes straightforward to calculate the GH shift for the TE mode and for the TM mode by Eq. (6).

The difference between the GH shifts for TE and TM modes can therefore be deduced as

$$\Delta L_{GH} = L_{GH}^{TE} - L_{GH}^{TM}, \quad (7)$$

with

$$L_{GH}^{TE} = \tan i_1 \frac{\int_{-h}^0 |U_{\perp} \cos \alpha x + V_{\perp} \sin \alpha x|^2 dx + |t_{\text{eval}}^{\perp}|^2 \frac{\delta}{2}}{|r_{\text{tot}}^{\perp}|^2},$$

$$L_{GH}^{TM} = \tan i_1 \frac{\int_{-h}^0 |U_{\parallel} \cos \alpha x + V_{\parallel} \sin \alpha x|^2 dx + |t_{\text{eval}}^{\parallel}|^2 \frac{\delta}{2}}{|r_{\text{tot}}^{\parallel}|^2}. \quad (8)$$

The different parameters are explained in Appendix B. The difference between the two polarization states is important since it allows a direct comparison with the experimental results, as detailed in the following. Finally, it can be pointed out that only negligible differences appear on the calculated GH shift deduced for the total internal reflection on a thin dielectric film between the two methods and that the two curves corresponding to the two models are completely overlapped in Fig. 5. Following Renard's model and formulas (6)–(8), the GH shift results from two main contributions:

1. the Poynting's vector into the film, which corresponds to a guided mode near a resonance,
2. the Poynting's vector corresponding to the evanescent wave.

It is clear that, as soon as a resonance appears in the film, the resulting guiding effect significantly increases the displacement. In this case, the main contribution is due to the first part of Eq. (6). Of course, the second term due to the evanescent wave also shows a resonance but its magnitude is very small compared with that due to the first term. On the other hand, far away from any resonance, the second part corresponds to the classical GH shift already mentioned. Moreover, it is obvious starting

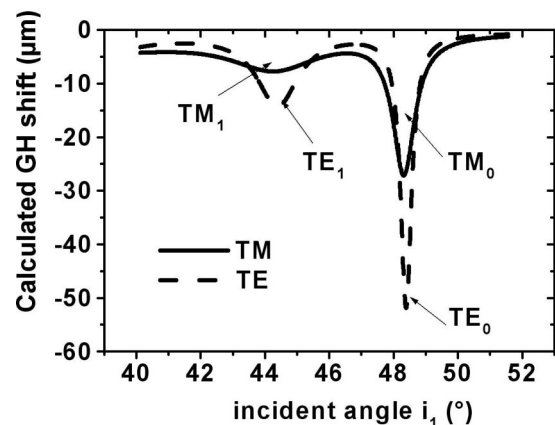


Fig. 5. Calculated GH shift by Artmann's or Renard's models versus the incidence angle for two polarization eigenstates: TE mode, TM mode.

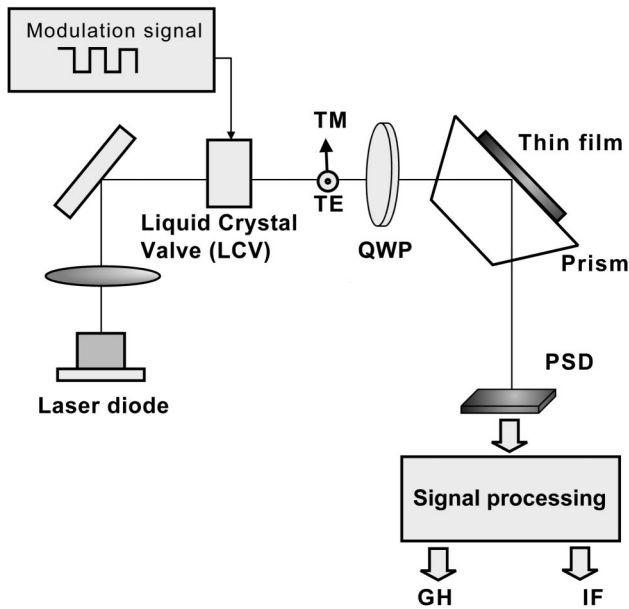


Fig. 6. Experimental setup used to measure the GH and IF shifts on a thin dielectric layer.

from Fig. 4 that, as soon as the amplitude of the electric field for  $TE_0$  is higher than it is for  $TE_1$ , the GH shift should be higher for  $TE_0$  compared to  $TE_1$  (see Fig. 5). These different specific behaviors will be further elucidated and compared to theory below.

For any other polarization states (elliptical or circular), it is also possible to calculate the GH shift based on Renard's model by the following technique. The incident electric field is decomposed as a linear combination on the basis of the two orthogonal polarized states TE and TM. Then the electric and magnetic fields into the thin film and into the air can be deduced by the approach already described in Appendixes A and B. Finally the Poynting's vectors into the film and in the air may be expressed. By use of Eq. (6), it becomes possible to calculate the GH shift for any intermediate state. Moreover, it is possible to calculate the transverse IF shift that also appears for an elliptical (or circular) polarization state by

$$L_{IF} = \frac{1}{\langle \Sigma_{rx} \rangle} \left( \int_{-h}^0 \langle \Sigma_{2y} \rangle dx + \int_{-\infty}^{-h} \langle \Sigma_{3y} \rangle dx \right). \quad (9)$$

Equation (9) must be related to Eq. (9) in Ref. 7 and will be useful to calculate the transverse IF shift when, instead of linearly polarized light, the thin film is periodically illuminated with a left- or right-handed circularly polarized beam.

### 3. EXPERIMENTAL RESULTS

To measure precisely the polarization dependence of such enhanced GH shift, we used the experimental setup already described elsewhere.<sup>5,7</sup> This setup is represented in Fig. 6 and will be only briefly described here. The collimated beam is emitted by a Spectra Diode Laboratories laser diode (model 6702 H1;  $\lambda=1.083 \mu\text{m}$ ) driven by a Spectra Diode Laboratories power supply (model SDL 800). With a birefringent Glan-Thomson prism, the linear

polarization state emitted by the laser diode is further improved to obtain a high polarization extinction ratio ( $>40 \text{ dB}$ ). The light beam passes through a LCV from Displaytech, Inc., (model LV1300) to periodically switch its polarization state. The valve allows periodic polarization switching between TE and TM modes. By locating a quarter-wave plate (QWP) just after the LCV, it also becomes possible to obtain circularly or elliptically polarized states before entering the prism. If the angle of incidence on the prism is close to  $0^\circ$ , the polarization state remains unchanged after transmission through the entrance interface; therefore, it also becomes the incident polarization states on the thin film.

The beam is totally reflected at the base of a specially designed prism [see Fig. 3(a)]. The substrate is made of a high-refractive-index glass ( $n_1=1.9$ ) while the base of the prism is covered with a thin, porous silicate film with a refractive index  $n_2=1.45$ . The thickness  $h$  is  $1.68 \mu\text{m}$ . The incidence angle is precisely controlled with a rotation stage. After the total reflection at the prism, the average beam position is photodetected by a two-dimensional PSD (Advanced MicroElectronics/UDT Sensors, Inc., model FIL-C4DG) that allows the simultaneous observation and measurement of both longitudinal and transverse shifts.

Because the resonant angles are slightly different between TE and TM modes (corresponding to the effect of polarization dispersion of the optical guide), the resonance peaks are not exactly coincident. Moreover, their amplitudes are different. The present technique allows measuring the difference between the GH shifts for TE and TM polarization states. The measured relative GH displacement is represented in Fig. 7. The abscissa shows the angular orientation representing the internal incidence angle compared with the axis normal to the base on which the thin film is deposited. The measured points show clearly identifiable peaks corresponding to the angular condition for a leaky guided mode into the planar dielectric film. Compared with the theoretical curve obtained by use of formulas (5)–(8), the experimental results are in good agreement with theory and correctly reproduce the observed structures as well as the amplitude of the resonance.

As can be deduced from a comparison between Fig. 5 and Fig. 7, the difference between the GH shift for TE and

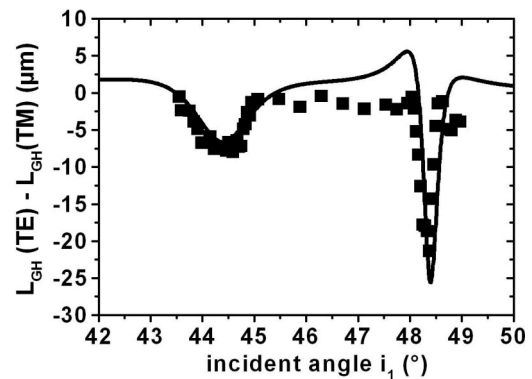


Fig. 7. Difference between the GH shifts for TE and TM polarization states versus the incidence angle on the thin film: comparison between theory (solid curve) and experiment (filled squares).

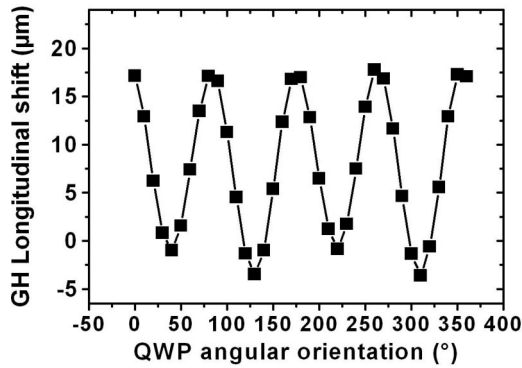


Fig. 8. Longitudinal shift measured versus the angular orientation of the QWP located in front of the LCV; measured for  $i_1 = 48.5^\circ$  corresponding to the first resonance peak.

TM modes is smaller than the absolute displacement. Of course, this result is not very surprising because, as already mentioned, the difference between the resonance angles is very small. The difference can be observed only when the electromagnetic field into the thin film is studied versus the incidence angle. As the amplitude of the GH shift is smaller for TM compared with TE polarization states, the experimental spatial shift observed corresponds mainly to the GH shift for the TE mode. For example, the maximum absolute GH shift for the  $TE_0$  mode is about  $55 \mu\text{m}$ , whereas it is only about  $30 \mu\text{m}$  for the  $TM_0$  mode. The relative GH shift between  $TE_0$  and  $TM_0$  is only  $25 \mu\text{m}$  but it matches relatively well the observed displacement. Even though the difference is smaller than the absolute displacement, it is still perfectly measurable with our technique, and the resonance peaks corresponding to the modes ( $TE_0$ – $TM_0$  and  $TE_1$ – $TM_1$ ) can be easily identified in Fig. 7. Moreover, it appears that when the order  $n$  of the leaky guided mode  $TE$ – $TM_n$  increases, the absolute (as well as the relative) GH shifts decrease. This is expected because when the order increases, the amplitude of the electromagnetic field decreases inside the thin film as is shown in Fig. 4 for  $TE_0$  and  $TE_1$ . Therefore, the amplitude of the associated Poynting's vector  $\Sigma_{2z}$  also decreases and it is straightforward, with Eq. (6), to see that the GH shift will become smaller. On the other hand, the width of the resonant peak becomes larger when the order  $n$  increases. For example, on the present thin film, the angular tolerance, defined as the FWHM of the resonance peak is  $\Delta i_1 = 0.8^\circ$  for ( $TE_0$ – $TM_0$ ) and  $\Delta i_1 = 2^\circ$  for ( $TE_1$ – $TM_1$ ).

To check that the displacement measured is undoubtedly attributed to the GH effect and not to a spurious effect, the QWP just after the LCV was turned around its axis and the corresponding longitudinal shift was measured versus the angular orientation of the QWP, and therefore versus the incident polarization states. The results are shown in Fig. 8. In particular, the periodicity observed corresponds to the expected value. As soon as the neutral axes of the QWP are oriented along the linear polarization states emerging from the LCV, a maximum longitudinal shift is observed. This is not surprising since in this case the polarization states correspond to  $TE$ – $TM$ , the two polarization eigenstates of the planar waveguide. Therefore, a guiding effect becomes possible (as long as

the incidence angle also corresponds to a resonant one). On the other hand the effect is nullified when the incident polarization states are circular, that is to say when the neutral axes of the QWP are oriented at  $45^\circ$  compared with those of the LCV. This behavior has previously been observed for the GH shift on a single interface and was recognized as a good way to check the viability of the measured effect.

As already mentioned, the IF shift can also be observed when a circularly polarized beam is totally reflected on a dielectric interface. One may wonder whether some peculiar behavior such as guiding effects could be observed on a thin film deposited on a substrate. While the longitudinal GH shift can be described using either Artmann's or Renard's models, the theoretical description of the IF shift on thin film is possible only by use of Renard's model. Without going too much into details, the technique used is basically similar to the method already described in Ref. 7 for a single interface. And because the PSD used during our experiment has a two-dimensional structure, it allows the simultaneous measurement of both the longitudinal and the transversal shifts. Therefore, rotating the QWP at  $45^\circ$  allows periodic switching of the polarization state between  $\sigma^+$  and  $\sigma^-$ . In the event the circular polarization states are not strictly speaking polarization eigenstates for a dielectric optical waveguide, it is obvious that no real guiding effect could be expected. However, when the lateral displacement between  $\sigma^+$  and  $\sigma^-$  is calculated versus the incidence angle, some peculiar structures are predicted as are represented on the theoretical curve shown in Fig. 9.

The experimental points measured in the transverse direction are in relatively good agreement with the theory, especially if we consider the order of magnitude of the observed effect. However, it becomes more difficult to identify clearly the predicted structure when considering the experimental points. To check further that the observed experimental shift can actually be attributed to the IF effect, the transverse displacement was also measured versus the angular orientation of the QWP. First, the amplitude of the transverse shift appears in quadrature with the longitudinal shift, which is exactly what is expected theoretically. Moreover, the periodicity is half that observed for the longitudinal shift because the sign of the relative lateral displacement reverses between

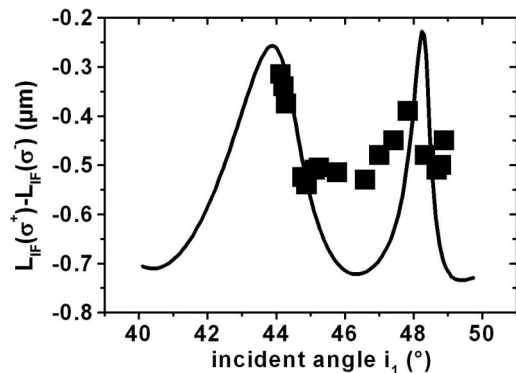


Fig. 9. Difference between the IF shift for  $\sigma^+$  and  $\sigma^-$  polarization states versus the incidence angle on the thin film; comparison between theory (solid curve) and experiment (filled squares).

$\sigma^+ - \sigma^-$  and  $\sigma^- - \sigma^+$ . If the amplitude of the transverse shift on a thin dielectric film is compared with the same effect observed on a single interface, the orders of magnitude are almost the same with no specific enhancement attributed to the film structure.

To understand better the theoretical results obtained for the IF effect on a thin dielectric film, we have decomposed the calculated transverse shift into two terms. The first represents the flux of the Poynting's vector into the thin film. This term could be considered as the contribution of the geometrical part of the shift due to multiple reflections inside the thin film. The second part is due to the evanescent wave in the air surrounding the film. It corresponds to the effect also observed on a single interface, except that the electric field into the thin film replaces the incident field and could be significantly enhanced as a result of the guiding effects into the structure. Figure 10 represents the two contributions as well as the resulting total transverse shift, which was already shown in Fig. 9. Such decomposition allows us to see clearly that the two contributions have opposite sign, which means that they partly compensate for each other. On the other hand, it shows that the two contributions present similar structures (with the exception of the opposite sign) and reveals that some form of guiding must appear even when using circularly polarized light.

To confirm this guiding effect, the absolute longitudinal shift has been calculated for circularly polarized light and reveals a strong resonance as soon as the incidence angle corresponds to the guided modes's TE or TM. Of course, this longitudinal shift can not be directly observed with our experimental setup because the longitudinal shifts are equal for the two orthogonal polarized  $\sigma^+ - \sigma^-$  states. For circularly polarized light, the transverse shift is not enhanced in the waveguide structure, even when the light is physically guided inside the film. The reason for this peculiar behavior is that the polarization state will be modified along the guide each time the light is totally reflected at the film-air interface. At the beginning if the transverse shift is positive, it becomes negative after only

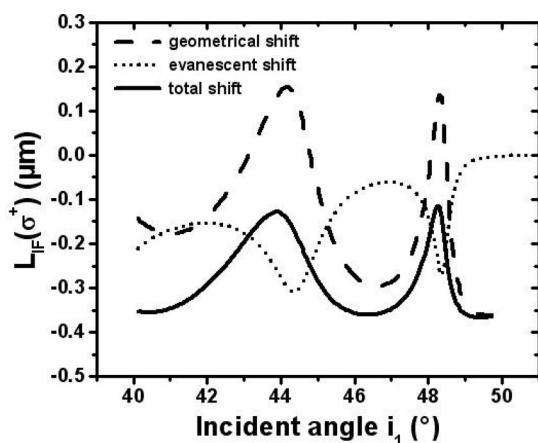


Fig. 10. The two contributions for the Imbert-Fedorov shift attributed, respectively, to (a) the multiple reflections inside the thin film (dashed curve), (b) the evanescent wave along the film-air interface (dotted curve). The solid curve represents the sum of the two contributions and should be compared with the experimental results.

a few reflections. Therefore, the transverse shift is periodically counterbalanced and no enhancement could be expected.

This modification of the polarization states during each total internal reflection is especially pronounced in our case because we are far away from the critical angle. On the other hand the longitudinal displacement is always positive and therefore can not be cancelled as a result of the modification of the polarization state during propagation. This will lead to a strong enhancement of the longitudinal displacement as soon as the light is guided, because it will benefit from the cumulative effect in the case of multiple reflections. In fact, only the structured dependence of the transverse displacement versus the angular orientation should be considered as the peculiar behavior for the IF effect on thin film. Therefore, further development would be necessary to identify fully the predicted structure.

One way to improve the identification of the peculiar effects attributed to the thin film is to choose a specific structure to enhance further the guiding properties. Therefore, let us consider the main parameters that can have an influence on the GH shift and quantify their effects on the order of magnitude of the displacement. The thickness  $h$  of the layer, the refractive index  $n_1$  of the substrate, and the distributed losses into the thin film could have significant influence on the guiding properties of the layer and therefore on the resulting GH displacement. We have decided to keep constant the refractive index of the layer because the resulting effect is very similar to a modification of the refractive index of the substrate. The most sensitive parameter is the thickness  $h$  of the layer, mainly because it can be modified in a wide range. When it is increased the number of allowed eigenmodes into the thin film becomes higher and the resonance angles corresponding to the successive orders become closer. This result is expected because, as soon as the thickness increases, the multimode character of the waveguide becomes more pronounced. Moreover, a thicker waveguide means correspondingly more energy stored in the layer and a larger amplitude for the resulting displacement. For example, when the thickness increases from  $h = 1.7 \mu\text{m}$  to  $3.4 \mu\text{m}$ , the absolute amplitude of the GH shift increases from  $55 \mu\text{m}$  to  $550 \mu\text{m}$  for the  $\text{TE}_0$  mode. However, the resonance condition becomes more sensitive to the incidence angle and the peaks become narrower. Therefore, the present thin film is a good compromise between a well-pronounced resonance and a relatively wide angular acceptance.

The other important parameter is the difference between the refractive indices of the film and the substrate. When the contrast becomes higher, the finesse of the Fabry-Perot interferometer corresponding to the thin film increases. Therefore, when the refractive index  $n_1$  of the substrate significantly increases above  $n_2$ , the GH shift becomes higher, and simultaneously each resonant peak becomes narrower. Moreover, with any increase of  $n_1$ , the range between the total reflections on the film-air and substrate-film interfaces becomes narrower, but not so much as to cause difficulties in observing the effect. Once again the refractive index  $n_1 = 1.9$  seems a relatively good compromise to get enough con-

trast between the substrate and the film to increase the GH shift.

Finally, the distributed losses could also have a significant influence on the amplitude of the resonance but only if the losses become high (typically a few percent per round trip into the layer). Because the thickness of the film is limited to a few micrometers the losses should also have limited impact on the amplitude of the resonance peak.

However, this investigation is mainly theoretical and it is still necessary to check experimentally the effect of possible adjustments of the main parameters such as thickness  $h$  or index  $n_1$ .

## 4. CONCLUSION

In the present paper, the geometrical displacement that accompanies a totally reflected light beam onto a thin dielectric film is studied. In the particular case of a thin film with a refractive index lower than that of the substrate on which it is deposited, it is demonstrated both theoretically and experimentally that under specific incidence angles, the longitudinal GH shift presents some resonance peaks that strongly depend on the internal structure of the dielectric layer. These peaks correspond to the leaky guided eigenmodes of the planer waveguide. The experimental setup, previously used to measure GH and IF effects on a single interface, is based on a periodic polarization switching technique. In fact, it permits measuring only the difference between the TE and TM shifts, but it is perfectly adapted to characterize fully the resonance due to the differences between the two polarization eigenstates.

The transverse IF shift was also observed and measured versus the incidence angle. The experimental transverse shift presents no resonance, thus confirming the theoretical calculations made by use of Renard's model. However, some peculiar structures versus the incidence angle—not observed in the case of a single interface—are predicted in such dielectric thin film. These dependences tend to appear on the measured curves, but improvements in methods are needed to identify them better.

The evanescent wave near a thin dielectric film has long been recognized as an interesting tool to measure a chemical or biological reaction near the interface. Usually the detection is based on interferometric techniques. Our approach, developed initially to observe and measure the GH or IF shifts, could also be useful for optical sensing. It consists of detecting a spatial shift instead of a phase shift and could be very sensitive, especially when coupled to a thin-film structure observed near a resonance. Moreover, other structures presenting giant or unusual GH shifts could also be investigated with the present technique, such as the effects predicted at an interface with right-handed and left-handed materials (or negative refractive index).<sup>15,16</sup>

## APPENDIX A: EXPRESSIONS FOR THE ELECTROMAGNETIC FIELD AND RESULTING POYNTING'S VECTOR

### 1. For the Reflected Wave in the Substrate

The complex amplitude  $E_r$  of the reflected wave on the interface between substrate and film ( $x=0$ ) can be ex-

pressed by use of Eq. (3). Therefore, the Poynting's vector associated with the reflected beam can be directly deduced from

$$\Sigma_r = \frac{n_1 E_0^2}{2\mu_0 c} |r_{\text{tot}}|^2 \begin{pmatrix} \cos i_1 \\ 0 \\ \sin i_1 \end{pmatrix}, \quad (\text{A1})$$

where  $E_0$  is the incident electric field,  $n_1$  is the refractive index in the substrate,  $\mu_0$  is the magnetic permeability of vacuum,  $c$  is the velocity of light, and  $r_{\text{tot}}$  is the total reflection coefficient defined by use of Eq. (3).

### 2. For the Evanescent Wave in the Air

With an approach similar to that used to calculate the reflected electric field, the thin dielectric layer could be considered a Fabry–Perot interferometer, and a transmission coefficient  $t_{\text{eva}}$  for the evanescent wave can be calculated to obtain the amplitude of the electric field at the interface between the layer and the air. The evanescent wave being inhomogeneous, its amplitude decreases exponentially when the coordinate  $x$  decreases from  $-h$  to  $-\infty$ . The corresponding Poynting's vector for the evanescent wave becomes simply

$$\Sigma_3 = \frac{n_3 E_0^2}{2\mu_0 c} |t_{\text{eva}}|^2 \exp\left[\frac{2(x+h)}{\delta}\right] \begin{pmatrix} 0 \\ 0 \\ \frac{n_1}{n_3} \sin i_1 \end{pmatrix}, \quad (\text{A2})$$

where  $\delta$  is the penetration depth defined exactly as for a classical total reflection for a single interface,<sup>7</sup> and  $t_{\text{eva}}$  depends on the incident polarization states (TE or TM).

## APPENDIX B: EXPRESSIONS FOR THE ELECTROMAGNETIC FIELD AND THE RESULTING POYNTING'S VECTOR INTO THE THIN DIELECTRIC LAYER

The electric and magnetic fields into the thin dielectric layer are respectively called  $\mathbf{E}_2$  and  $\mathbf{B}_2$ , and they can be calculated by assuming the superposition of a descendant wave and an ascendant wave into the structure. The wave vectors associated with these two waves are, respectively,

$$\mathbf{k}_2^{\text{d}} = \begin{pmatrix} -\alpha \\ 0 \\ \beta \end{pmatrix},$$

$$\mathbf{k}_2^{\text{a}} = \begin{pmatrix} \alpha \\ 0 \\ \beta \end{pmatrix}, \quad (\text{B1})$$

with  $\alpha = (2\pi/\lambda)n_2 \cos i_2$  and  $\beta = (2\pi/\lambda)n_2 \sin i_2$ . Two polarization eigenstates for a planar optical waveguide must be distinguished: the TE mode with the electric field oriented along the  $y$  axis and the TM mode with the magnetic field along the  $y$  axis.

### 1. Case of TE Mode

Starting with the hypothesis that the electric field can be described as

$$\mathbf{E}_2 = E_0(U_{\perp} \cos \alpha x + V_{\perp} \sin \alpha x) \times \exp[-j(\omega t - \beta z)] \times \begin{pmatrix} 0 \\ 1 \\ 0 \end{pmatrix}. \quad (\text{B2})$$

It is straightforward to express the magnetic field  $\mathbf{B}_2$  by use of the Maxwell's equation  $\text{Curl}(\mathbf{E}) = -\partial\mathbf{B}/\partial t$ . We have

$$\mathbf{B}_2 = \begin{cases} -\frac{E_0}{c} n_2 \sin i_2 (U_{\perp} \cos \alpha x + V_{\perp} \sin \alpha x) \\ \times \exp[-j(\omega t - \beta z)] \\ 0 \\ -j\frac{E_0}{c} n_2 \cos i_2 (-U_{\perp} \cos \alpha x + V_{\perp} \sin \alpha x) \\ \times \exp[-j(\omega t - \beta z)] \end{cases}. \quad (\text{B3})$$

The continuity of components at the interface between layer and air imposes the following boundary conditions:

$$\begin{aligned} E_{2y}(-h) &= E_{3y}(-h), \\ \mathbf{B}_{2z}(-h) &= B_{3z}(-h), \end{aligned} \quad (\text{B4})$$

and the constants  $U_{\perp}$  and  $V_{\perp}$  can be deduced as

$$\begin{aligned} U_{\perp} &= t_{\text{eva}}^{\perp} \left\{ \cos \alpha h + \frac{n_3}{n_2 \cos i_2} \left[ \left( \frac{n_1}{n_3} \sin i_1 \right)^2 - 1 \right]^{1/2} \right. \\ &\quad \left. \times \sin \alpha h \right\}, \\ V_{\perp} &= t_{\text{eva}}^{\perp} \left\{ -\sin \alpha h + \frac{n_3}{n_2 \cos i_2} \left[ \left( \frac{n_1}{n_3} \sin i_1 \right)^2 - 1 \right]^{1/2} \right. \\ &\quad \left. \times \cos \alpha h \right\}. \end{aligned} \quad (\text{B5})$$

The resulting associated Poynting's vector can be calculated by  $\Sigma_2 = 1/2\mu_0 \text{Re}(\mathbf{E}_2 \times \mathbf{B}_2^*)$  and can be expressed versus the parameters  $U_{\perp}$  and  $V_{\perp}$  as

$$\Sigma_2 = \frac{E_0^2}{2\mu_0 c} n_1 \sin i_1 (U_{\perp} \cos \alpha z + V_{\perp} \sin \alpha z)^2 \times \begin{pmatrix} 0 \\ 0 \\ 1 \end{pmatrix}. \quad (\text{B6})$$

## 2. Case of TM Mode

Similarly, the magnetic field can be described as

$$\mathbf{B}_2 = \frac{n_2 E_0}{c} (U_{\parallel} \cos \alpha x + V_{\parallel} \sin \alpha x) \times \exp[-j(\omega t - \beta z)] \times \begin{pmatrix} 0 \\ 1 \\ 0 \end{pmatrix}. \quad (\text{B7})$$

It is straightforward to express the electric field  $E_2$  by use of the Maxwell's equation  $\text{Curl}(\mathbf{B}) = n_2^2/c^2 \partial\mathbf{E}/\partial t$ . We have

$$\mathbf{E}_2 = \begin{cases} E_0(U_{\parallel} \cos \alpha x + V_{\parallel} \sin \alpha x) \frac{n_1}{n_2} \sin i_1 \\ \times \exp[-j(\omega t - \beta z)] \\ 0 \\ jE_0 \cos i_2 (-U_{\parallel} \cos \alpha x + V_{\parallel} \sin \alpha x) \\ \times \exp[-j(\omega t - \beta z)] \end{cases}. \quad (\text{B8})$$

The continuity of components at the interface between layer and air imposes the following boundary conditions:

$$\begin{aligned} E_{2z}(-h) &= E_{3z}(-h), \\ B_{2y}(-h) &= B_{3y}(-h), \end{aligned} \quad (\text{B9})$$

and the constants  $U_{\parallel}$  and  $V_{\parallel}$  can be deduced as

$$\begin{aligned} U_{\parallel} &= t_{\text{eva}}^{\parallel} \left\{ \frac{n_3}{n_2} \cos \alpha h + \frac{1}{\cos i_2} \left[ \left( \frac{n_1}{n_3} \sin i_1 \right)^2 - 1 \right]^{1/2} \right. \\ &\quad \left. \times \sin \alpha h \right\}, \\ V_{\parallel} &= t_{\text{eva}}^{\parallel} \left\{ -\frac{n_3}{n_2} \sin \alpha h + \frac{1}{\cos i_2} \left[ \left( \frac{n_1}{n_3} \sin i_1 \right)^2 - 1 \right]^{1/2} \right. \\ &\quad \left. \times \cos \alpha h \right\}. \end{aligned} \quad (\text{B10})$$

The resulting associated Poynting's vector can be calculated by use of  $\Sigma_2 = 1/2\mu_0 \text{Re}(\mathbf{E}_2 \times \mathbf{B}_2^*)$  and can be expressed in terms of  $U_{\parallel}$  and  $V_{\parallel}$  as

$$\Sigma_2 = \frac{E_0^2}{2\mu_0 c} n_1 \sin i_1 (U_{\parallel} \cos \alpha z + V_{\parallel} \sin \alpha z)^2 \times \begin{pmatrix} 0 \\ 0 \\ 1 \end{pmatrix}. \quad (\text{B11})$$

## ACKNOWLEDGMENTS

R. Kaiser thanks V. S. Bagnato, S. Muniz, and the Optics Center at Sao Carlos, University of Sao Paulo, for their help in the preparation of the coated prisms and their assistance during his stay in Sao Carlos.

Corresponding author S. Girards' e-mail address is sylvain.girard@ensicaen.fr.

## REFERENCES

1. F. Goos and H. Hänchen, "Ein neuer und fundamentaler Versuch zur Totalreflexion," *Ann. Phys.* **1**, 333–346 (1947).
2. F. Goos and H. Hänchen, "Neumessung des Strahlversetzungseffektes bei Totalreflexion," *Ann. Phys.* **2**, 87–102 (1949).
3. C. Imbert, "L'effet inertial de spin du photon: théorie et preuve expérimentale," *Nouv. Rev. Opt. Appl.* **3**, 199–208 (1972).
4. F. Bretenaker, A. Le Floch, and L. Dutriaux, "Direct measurement of the optical Goos–Hänchen effect in lasers," *Phys. Rev. Lett.* **68**, 931–933 (1992).
5. H. Gilles, S. Girard, and J. Hamel, "A simple measurement technique of the Goos–Hänchen effect using polarization

- modulation and position sensitive detector,” *Opt. Lett.* **27**, 1421–1423 (2002).
6. F. I. Fedorov, “К теории полного отражения,” *Dokl. Akad. Nauk SSSR* **105**, 465–468 (1955).
  7. F. Pillon, H. Gilles, and S. Girard, “Experimental observation of the Imbert-Fedorov transverse displacement after a single total reflection,” *Appl. Opt.* **43**, 1863–1869 (2004).
  8. Y. Levy and C. Imbert, “Amplification des déplacements à la réflexion totale,” *Opt. Commun.* **13**, 43–47 (1975).
  9. O. Costa de Beauregard, C. Imbert, and Y. Lévy, “Observation of shifts in total reflection of a light beam by a multilayered structure,” *Phys. Rev. D* **15**, 3553–3562 (1977).
  10. R. Kaiser, Y. Levy, J. Fleming, S. Muniz, and V. S. Bagnato, “Resonances in a single thin dielectric layer: enhancement of the Goos–Hanchen shift,” *Pure Appl. Opt.* **5**, 891–898 (1996).
  11. R. Kaiser, Y. Lévy, N. Vansteenkiste, A. Aspect, W. Seifert, D. Leipold, and J. Mlynek, “Resonant enhancement of evanescent waves with a thin dielectric waveguide,” *Opt. Commun.* **104**, 234–240 (1994).
  12. K. Artmann, “Berechnung der Seitenversetzung des totalreflektierten Strahles,” *Ann. Phys.* **2**, 87–102 (1948).
  13. R. H. Renard, “Total reflection: A new evaluation of the Goos–Hänchen shift,” *J. Opt. Soc. Am.* **54**, 1190–1197 (1964).
  14. M. Born and E. Wolf, *Principles of Optics*, 7th ed. (Cambridge U. Press, Cambridge, UK, 1999).
  15. P. R. Berman, “Goos–Hänchen shift in negatively refractive media,” *Phys. Rev. E* **66**, 067603–1/3 (2002).
  16. I. V. Shadrivov, A. A. Zharov, and Y. S. Kivshar, “Giant Goos–Hänchen effect at the reflection from left-handed metamaterials,” *Appl. Phys. Lett.* **83**, 2713–2715 (2003).